Subpicosecond magnetization dynamics in TbCo alloys

Sabine Alebrand, Ute Bierbrauer, Michel Hehn, Matthias Gottwald, Oliver Schmitt, Daniel Steil, Eric E. Fullerton, Stephane Mangin, Mirko Cinchetti, Martin Aeschlimann

Subpicosecond magnetization dynamics in TbCo alloys

Sabine Alebrand,[1] Ute Bierbrauer,[1] Michel Hehn,[2] Matthias Gottwald,[3,2] Oliver Schmitt,[1] Daniel Steil,[1] Eric E. Fullerton,[3] Stéphane Mangin,[2,3] Mirko Cinchetti,[1,*] and Martin Aeschlimann[1]

[1]*Department of Physics and Research Center OPTIMAS, University of Kaiserslautern, 67653 Kaiserslautern, Germany*

[2]*Institut Jean Lamour UMR CNRS 7198—Université de Lorraine, Vandoeuvre-lès-Nancy, France*

[3]*Center of Magnetic Recording Research, University of California San Diego, La Jolla, California 92093, USA*

(Received 17 October 2013; revised manuscript received 7 March 2014; published 3 April 2014)

Since the discovery of all-optical magnetization switching in rare-earth transition-metal alloys the underlying magnetization dynamics of multisublattice magnets has become a hot topic of modern magnetism. We studied the ultrafast magnetization dynamics in TbCo alloys as a function of the alloy composition and the laser fluence using either 800 nm or 400 nm probe pulses. Direct comparison between TbCo samples with different compositions for equal excitation conditions demonstrates that the magnetization dynamics of the Co sublattice strongly depends on the Tb concentration. For $Tb_{32}Co_{68}$ the magnetization of the sublattices can even transiently be reversed on a subpicosecond time scale.

DOI: 10.1103/PhysRevB.89.144404 PACS number(s): 75.78.Jp, 75.60.Jk, 75.50.Gg

I. INTRODUCTION

Rare-earth (RE)–transition-metal (TM) alloys are interesting materials both for fundamental research and for technological applications. They have been extensively studied to provide materials for magneto-optical recording and the permanent magnet industry. The magnetization of the alloy results from the magnetization of the RE and the TM sublattices. For some RE elements, called heavy rare earths, the magnetizations of the two sublattices are exchange coupled antiferromagnetically and the alloys are called ferrimagnetic as the sublattice magnetizations have different magnitudes.

The ability to switch the magnetization in RE-TM alloys either by laser heating above the Curie temperature T_{Curie} and subsequent cooling in an external applied magnetic field (thermomagnetic writing) or by laser heating above the magnetic compensation point (compensation point writing) has been investigated in manifold publications already since more than 20 years [1–7]. However, this material class has attracted new attention [8–15] since Stanciu *et al*. discovered in 2007 that it is even possible to deterministically switch the magnetization in RE-TM alloys (e.g., in GdFeCo) without an external applied magnetic field by using circularly polarized femtosecond laser pulses [called all-optical switching (AOS)]. Very recently, it was also shown that AOS can be observed for various RE-TM systems such as TbCo, TbFe, DyCo, HoCo alloys, Tb/Co and Ho/Co multilayers, as well as synthetic ferrimagnets [16]. Additionally, in 2012 magnetization switching with single linearly polarized laser pulses was demonstrated [17] in GdFeCo thin films. In Ref. [17], Ostler *et al*. theoretically attributed the observed switching with linearly polarized light to differences in the ultrafast magnetization dynamics of the two antiparallel coupled magnetic sublattices (i.e., Gd and FeCo) after laser excitation. Experimentally, such differences in the magnetization dynamics of the Gd- and Fe- sublattice had indeed been observed by Radu *et al*. one year earlier [18]. They showed that both magnetic sublattices can reverse their magnetization, whereby Fe reverses much faster than Gd, leading to a so-called transient ferromagneticlike state. For pure Fe and Gd samples, magnetization switching without an external magnetic field has up to now not been reported, showing that the elemental magnetization dynamics seems to be very different in a ferrimagnetic compound. These results brought the ultrafast magnetization dynamics after excitation with ultrashort laser pulses in ferrimagnetic systems into the focus of current research. In the following the magnetization decrease after laser excitation will be referred as demagnetization.

In general, understanding these multisublattice systems in detail is quite challenging: Element-selective experimental methods, like x-ray magnetic circular dichroism (XMCD) (as applied by Radu *et al*. in Ref. [18]) or higher-harmonics generation [19,20], can help to detect the sublattice-specific demagnetization while also new theoretical models are needed, taking into account the coupling of the magnetic sublattices [21,22]. However, quite recently Khorsand *et al*. suggested in Ref. [23] that for Tb-based alloys an element-selective probing of the magnetiztaion should also be possible using visible laser light.

In this paper we focus on the demagnetization of RE-TM alloys, whose understanding is a key to accessing the mechanism of all-optical switching. We investigate TbCo alloys and study the influence of the alloy composition and the laser fluence on the demagnetization dynamics, performing time-resolved magneto-optical Kerr-effect measurements with either blue (400 nm) or red (800 nm) probe pulses. We find that the sublattice magnetization quenching after laser excitation increases if the Tb concentration increases. For $Tb_{32}Co_{68}$ even transient magnetization reversal of the sublattices on a subpicosecond time scale is observed. We relate the increasing quenching of the Co sublattice with Tb concentration to two factors, namely, the increase of spin-orbit coupling and the decrease of the Co-Co exchange coupling with increasing Tb concentration. Furthermore, we can conclude that the dynamics of the Co and the Tb sublattice take place on a very similar time scale. Therefore, a transient ferromagneticlike state as observed in GdFeCo [18] could exist only in a quite narrow time interval.

*cinchett@rhrk.uni-kl.de

II. MEASUREMENT METHODS AND SAMPLES

The measurements were performed in a typical pump-probe magneto-optical Kerr-effect (MOKE) setup. The optical pulses were delivered by an amplifier system, having a central wavelength of 800 nm and a pulse duration of around 60 fs at the sample position. The beam was split at a beam splitter into pump and probe beams. In our experiments the probe beam either had a central wavelength of 800 nm (1.55 eV photon energy) or it was frequency doubled in a β-barium borate crystal (400 nm, 3.1 eV photon energy). By means of a delay line the pump and probe pulses could be temporally delayed. The probe beam was focused onto the sample down to a diameter of around 100 μm, which is much smaller than the size of the pump beam (around 2.6 mm in diameter) to ensure homogeneous excitation conditions at the position of the probe beam. The intensity of the pump beam could be varied by means of the combination of a half-wave plate and a polarizer up to around 5.5 mJ/cm^2.[1] The experiments were all performed in polar geometry, meaning that pump and probe pulses impinge on the samples at nearly normal incidence. After reflection on the sample the magnetization-dependent polarization rotation of the probe pulses was measured with a balanced photodiode detector. To exclude optical artifacts the measurements were performed for two external magnetic fields of opposite direction (strong enough to saturate the sample magnetization) and afterwards these two signals were subtracted to obtain the magnetization dynamics curves as presented in the figures below. All measurements were recorded at room temperature (RT).

The studied TbCo samples are multilayers, consisting of glass/ Ta(5 nm)/ Tb_xCo_{1-x}(20 nm)/ Cu(2 nm)/ Pt(5 nm). They were grown by dc magnetron sputtering at a base pressure lower than 5×10^{-9} mbar to ensure oxygen-free films. The TbCo alloys were grown by cosputtering Co and Tb from two separate targets. In detail, we have grown and investigated three samples of different compositions: $Tb_{12}Co_{88}$, $Tb_{26}Co_{74}$, and $Tb_{32}Co_{68}$, therefore varying the Tb concentration in a rather large range of 20%. For all compositions presented in this paper, the amorphous alloys are ferrimagnetic with perpendicular anisotropy. For the low (high) Tb concentration, that is to say $Tb_{12}Co_{88}$ ($Tb_{32}Co_{68}$), the net magnetization is along the Co (Tb) sublattice for all temperatures below the Curie temperature. However, for $Tb_{26}Co_{74}$ a compensation temperature may be defined ($T_{comp} \approx 500$ K) for which the magnetization is zero. At this temperature the net magnetization changes from parallel (below T_{comp}) to antiparallel (above T_{comp}) with respect to the Tb magnetization. In general, if the net magnetization at given ambient temperature is parallel to the Co (Tb) sublattice the alloy is called Co (Tb) dominant. As for all samples the magnetization is pointing out of plane, it enables us to measure them in an identical experimental geometry. Finally, note that the samples are the same that we used for the AOS studies in Ref. [12]. That means in particular that at RT only $Tb_{26}Co_{74}$ shows AOS.

[1]Due to inhomogeneities in the spot profile the exact value of all cited pump fluences by trend might be higher, but the order of magnitude remains valid.

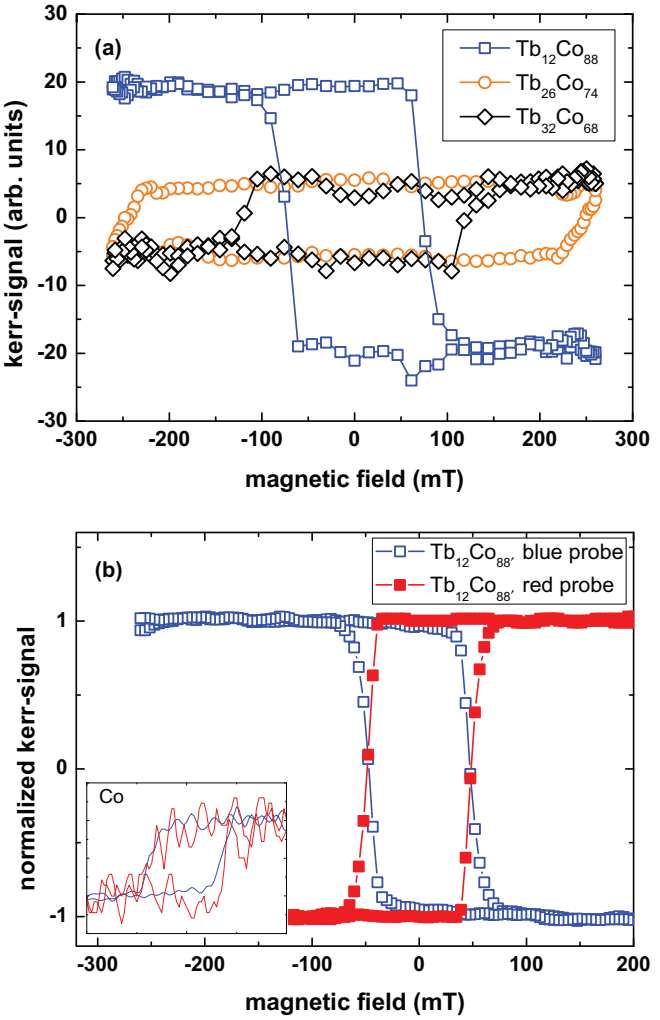

FIG. 1. (Color online) (a) Hysteresis loops of the different samples at room temperature measured with 400 nm laser pulses. The different hysteresis orientation demonstrates that $Tb_{12}Co_{88}$ is Co dominant, while $Tb_{26}Co_{74}$ and $Tb_{32}Co_{68}$ are Tb dominant. (b) Hysteresis loop for $Tb_{12}Co_{88}$ measured with either blue (400 nm) or red (800 nm) optical pulses. The inset shows the corresponding hysteresis loops for pure cobalt.

Figure 1(a) shows the static hysteresis loops of the three TbCo samples measured without pump pulse in polar geometry with a probe wavelength of 400 nm (static hysteresis). As we will discuss later in more detail, according to Ref. [23] the MOKE signal measured at 400 nm is mainly sensitive to the magnetization of the Tb sublattice. This means that Tb-dominant and Co-dominant compounds should show hysteresis with opposite directions at 400 nm. This is exactly what we observe in Fig. 1(a), where the samples $Tb_{26}Co_{74}$ and $Tb_{32}Co_{68}$, which are Tb dominant at RT, show a hysteresis with opposite orientation to that of the Co-dominant $Tb_{12}Co_{88}$ sample. In Fig. 1(a) we also observe that the coercive field is in the order of 75 mT for $Tb_{12}Co_{88}$ and 120 mT for $Tb_{32}Co_{68}$, but it is higher for $Tb_{26}Co_{74}$ ($\approx$250 mT). This is due to the fact that at RT $Tb_{26}Co_{74}$ is close to its compensation point, where the coercivity of a ferrimagnet

strongly increases. Furthermore, the rectangular shape of the hysteresis confirms that the samples show strong perpendicular magnetic anisotropy (PMA).

Additionally, we measured static hysteresis loops using probe pulses with a central wavelength λ of either 400 nm (blue) or 800 nm (red). We observe that the orientation of the hysteresis depends on the laser wavelength, as it is exemplarily shown for $Tb_{12}Co_{88}$ in Fig. 1(b). In general the 4*f* states of RE elements, which carry a significant amount of the magnetic moment, are located several eV below the Fermi energy. That is why most commonly it was assumed in the literature that the Kerr signal in the visible optical range results only from the TM sublattice. However, Khorsand *et al.* (Ref. [23]) recently demonstrated that the Tb sublattice can significantly contribute to the Kerr signal in Tb-based RE-TM alloys due to a strongly spin-orbit-split 4*f* state at approximately 2.4 eV below the Fermi energy, which can be excited with photon energies in the visible spectral range. In detail, they showed for a $Tb_{16}Fe_{75}Co_9$ alloy that at a laser wavelength of $\lambda = 800$ nm (photon energy 1.55 eV) the Kerr signal is dominated by the Co sublattice, while for $\lambda = 400$ nm (photon energy 3.1 eV) it is dominated by the Tb sublattice. As the Co and Tb sublattice are aligned antiparallel in our samples, this is in accordance with the hysteresis orientation change for blue (400 nm) and red (800 nm) light.

Nevertheless, the observed wavelength-dependent changes of the hysteresis loop might in principle also be attributed to a sign change of the Co sublattice's Kerr rotation. To check this, we measured the wavelength-dependent hysteresis loop for a pure Co sample [see inset Fig. 1(b)], but no changes of the hysteresis orientation were observed. Although the situation might be different in TbCo due to the different electronic states compared to pure Co, we assume in the following that we detect the Co sublattice magnetization if we probe with $\lambda = 800$ nm while the signal measured at $\lambda = 400$ nm is a superposition of the Co and Tb sublattice contributions, but it is dominated by the signal resulting from the Tb sublattice. We can therefore element-selectively probe the magnetization dynamics.

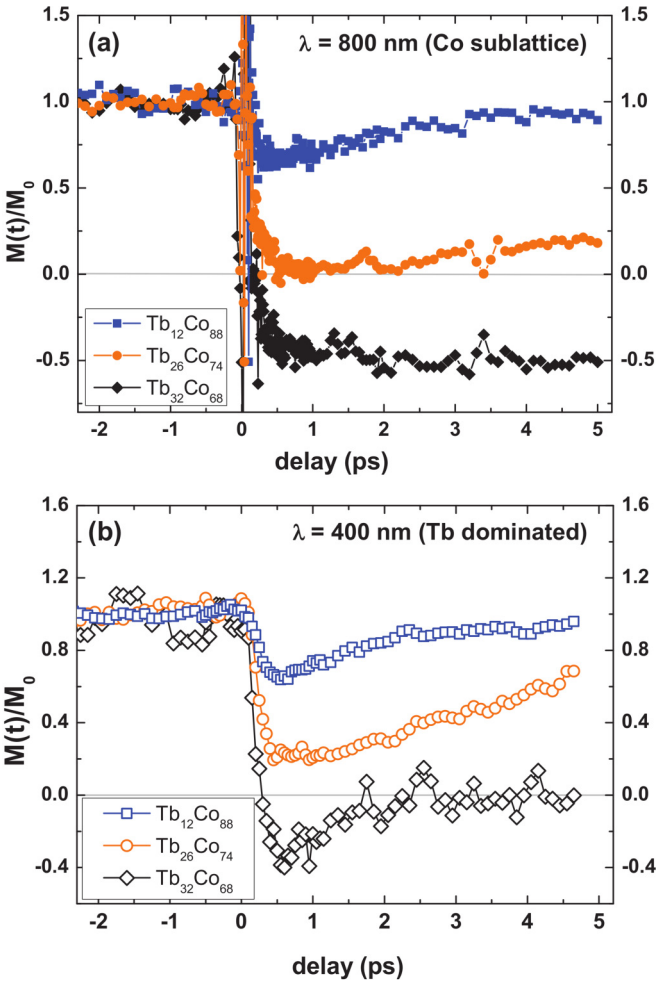

FIG. 2. (Color online) Time-dependent magnetization traces for three different TbCo compositions [$Tb_{12}Co_{88}$ (blue rectangles), $Tb_{26}Co_{74}$ (orange circles), and $Tb_{32}Co_{68}$ (black diamonds)] at the same excitation fluence. The magnetization is normalized to the value before delay time zero. (a) $\lambda = 800$ nm, excitation fluence 2.2 mJ/cm^2; (b) $\lambda = 400$ nm, excitation fluence 2.4 mJ/cm^2. The spikes around point zero in (a) are caused by optical artifacts due to the interference of the collinear impinging pump and probe beams having the same wavelength.

III. RESULTS AND DISCUSSION

A. Composition-dependent magnetization dynamics probed with λ = 800 nm: Dynamics of the cobalt sublattice

Figure 2(a) shows the time dependence of the MOKE signal following a given excitation (fluence 2.2 mJ/cm^2) for the three TbCo alloys discussed above. Here, the MOKE signal was probed with $\lambda = 800$ nm and reflects thus mainly the magnetization of the cobalt sublattice. The data are normalized to the signal value at negative delay. For all cases, an ultrafast quenching of the magnetization on the femtosecond time scale can be seen. Furthermore, if the Tb concentration within the alloy increases, the magnetization quenching increases too. Notably, for $Tb_{32}Co_{68}$ the magnetization transiently even becomes negative, meaning that the magnetization orientation has reversed.

A straightforward explanation for the different quenchings in TbCo at constant excitation fluence would be a different absorption for the three samples, leading to different effective excitation conditions. Therefore, we determined the absorption for all samples by measuring the incoming, transmitted, and reflected light intensity. The absorbed intensity is then determined as the difference between the incoming light and the sum of transmitted and reflected light. We found that for all samples the absorption is equal (≈30%) within error bars (≈3%). This excludes a different absorption as the reason for the large observed changes in magnetization quenching.

A further possible explanation for the composition dependence of the magnetization dynamics of the Co sublattice might be the different amounts of total Co magnetic moment for the three samples. Generally, one can estimate that for a sample with twice the magnetic moment, also twice as many spin flips are needed to obtain the same relative quenching. As can be seen in Fig. 2(a), at equal excitation fluence the

quenching is roughly three times as high for $Tb_{26}Co_{74}$ as for $Tb_{12}Co_{88}$. Considering that the Co magnetic moment per atom, μ_{Co}, will vary with Tb concentration [24],[2] we estimate that for equal spin-flip probability the quenching for $Tb_{26}Co_{74}$ should be a factor of 1.69 higher than for $Tb_{12}Co_{88}$. This corresponds to a quenching of ≈60% for $Tb_{26}Co_{74}$, which is nearly 40% less than observed experimentally. We conclude that the difference in magnetic moments will influence the composition-dependent demagnetization dynamics, but an exclusive explanation of the observed trend in terms of this difference is unlikely.

There are two additional factors which can support the observed trend in our measurements. These are (i) the change of the spin-orbit coupling with Tb concentration and (ii) the Tb-dependent Co-Co exchange coupling. Both these factors influence the cobalt magnetization directly but also through interaction between the Co and the Tb sublattices, as explained in the following.

Concerning factor (i), Tb is known to possess a large spin-orbit coupling due to its large orbital momentum of $L = 3$. This large spin-orbit coupling will lead to a high spin-flip probability α. Consequently, assuming that spin-flip processes play a significant role for the demagnetization in multisublattice magnets, equivalently to the demagnetization in 3*d* ferromagnets, the magnetization quenching should increase with increasing Tb concentration. This is consistent with our experimental observations. For GdFeCo the effect caused by the spin-orbit coupling is expected to be less pronounced. In fact, Gd is an *S* ion with zero orbital momentum of the 4*f* electrons, resulting in a weaker spin-orbit coupling than in Tb. Therefore, an increase in Gd concentration will only weakly affect the demagnetization behavior of GdFeCo, and additional influences like, e.g., the position of the compensation temperature can dominate the dynamics, as observed in Ref. [25]. Note that for our measurements the exact position of the magnetic compensation temperature T_{comp} might also influence the dynamics: We observe a higher quenching for samples having T_{comp} greater than RT. However, the variation for the quenching of our two samples with T_{comp} greater than RT is still quite pronounced, which indicates that additional factors must play a significant role.

Related to factor (ii), the variation of the Co-Co exchange coupling, it was shown in Ref. [26] that at least for GdCo the Co-Co exchange constant $J_{Co\text{-}Co}$ decreases with increasing Gd concentration, while the Gd-Co exchange constant $J_{Gd\text{-}Co}$ stays nearly constant. We expect a similar behavior for TbCo, since the composition-dependent change of the Curie temperature (which is determined by the exchange constants) is qualitatively independent of the RE element [27]. Furthermore we argue that the smaller $J_{Co\text{-}Co}$ at constant $J_{Tb\text{-}Co}$ the easier it should be to demagnetize the Co sublattice. Overall, the dependence of $J_{Co\text{-}Co}$ on the Gd concentration could explain the increasing trend of the magnetization quenching with increasing Tb concentration observed in our experiment.

[2]From Ref. [24] we estimate that μ_{Co} ($x = 26\%$) is roughly $0.7\mu_{Co}$ ($x = 12\%$).

B. Composition-dependent magnetization dynamics probed with λ = 400 nm: Dynamics of the terbium sublattice (Tb dominant)

In Fig. 2(b) the time-resolved demagnetization traces of the three TbCo samples measured at $\lambda = 400$ nm are shown. Recall that these signals are assumed to result from both the Co and the Tb sublattices, but are dominated by the Tb sublattice. Comparing Fig. 2(b) to Fig. 2(a), one directly recognizes the same composition-dependent trend of the magnetization quenching, i.e., the quenching of the Tb sublattice also increases with Tb concentration. Moreover, the recovery back to the initial magnetization state seems to take longer for $\lambda = 800$ nm compared to $\lambda = 400$ nm. However, a detailed discussion of the recovery dynamics is beyond the scope of this paper and we will focus only on the demagnetization and reversal dynamics in the following.

As a first conclusion, we point out here that the changes in magnetic moment cannot be responsible for the observed composition-dependent trend of the Tb sublattice's demagnetization: As Tb concentration increases the total magnetic moment of the Tb sublattice increases, too. Hence, for constant spin-flip probability this should result in the opposite concentration trend to that of the magnetization quenching. However, as discussed already above, the spin-flip probabilitiy is expected to increase with Tb concentration and might, in principle, explain the experimental observations.

Equivalently to the measurements performed with $\lambda = 800$ nm a transient magnetization reversal occurs for $Tb_{32}Co_{68}$. Note that in case of a larger demagnetization time τ of the Tb than of the Co sublattice, the magnetization reversal can result only from a real transient reversal of the Tb sublattice (at least, if one neglects possible changes of the Co sublattice's Kerr rotation upon laser heating). Otherwise, if $\tau_{Tb} < \tau_{Co}$ (which can be the case close to T_{Curie} [28]) the observed negative magnetization signal might also be related to the Co sublattice's contribution to the Kerr rotation at times where the Tb sublattice magnetization is already strongly quenched. Overall, and by comparing the results of Figs. 2(a) and 2(b) we conclude that the Tb sublattice quenches its magnetization on a similar time scale as the Co sublattice. In particular, both sublattices reverse their magnetization in less than 500 fs. This is in agreement with the findings of López-Flores *et al.* [29]. Consequently, a transient ferromagneticlike state suggested to be responsible for all-optical switching should appear only in a quite narrow time interval, in particular much smaller than for GdFeCo [18], where it takes around 1.5 ps until the magnetization of the Gd sublattice is fully quenched and reversal takes place. In this context, we point out that although we observe a transient magnetization reversal for both sublattices in $Tb_{32}Co_{68}$, AOS was not observed for this alloy composition [12].

Before we consider the influence of the exciting laser fluence on the occurrence of magnetization reversal in the next section, we discuss here the results presented in Secs. III A and III B in the light of ultrafast dynamics in multisublattice magnets with respect to single-element ferromagnets. In this regard, we point out that for a single-element ferromagnet demagnetization can occur due to energy and momentum dissipation between its electron, the spin, and the lattice system.

Such processes are referred to in Ref. [21] as relativistic (or spin-orbit-driven) effects. In contrast, in multisublattice magnets energy and angular momentum redistribution can additionally take place by exchange between the different sublattices (exchange-driven effects in Ref. [21]). In this regard, our results are consistent with such an exchange between the two sublattices as the composition-dependent trend is the same for Tb and Co. Furthermore, our results might also suggest that the exchange processes become stronger for higher Tb concentration. However, the fact that the exchange constant between the two sublattices ($J_{\text{Co-Tb}}$) is expected to be nearly independent of the alloy composition [26] does not support this conclusion. Nevertheless, note that corresponding to the model by Mentink *et al.* [21] the exchange-driven processes will dominate the reversal only in a situation where one sublattice is already completely quenched due to spin-orbit-driven effects while the other sublattice is still magnetized in its original orientation. Therefore, we point out that the similar demagnetization time scales for the Tb and Co sublattices observed in our measurements might even counteract the exchange-driven magnetization reversal. Instead, an enhancement of the spin-orbit-driven sublattice internal demagnetization (as addressed in Sec. III A, for example) will indirectly increase the significance of the exchange-driven effects. This demonstrates the complex interplay of spin-orbit- and exchange-driven effects in multisublattice magnets.

C. Fluence-dependent measurements

Finally, we investigate the composition-dependent ability of transient magnetization reversal in more detail. For $Tb_{32}Co_{68}$ we found that a transient magnetization reversal occurs only if the fluence is sufficiently high (data not shown here). Therefore, we performed fluence-dependent measurements for $Tb_{12}Co_{88}$ and $Tb_{26}Co_{74}$ to investigate if reversal can occur at higher fluence. As can be seen in Figs. 3(a) and 3(b) for $Tb_{12}Co_{88}$ the quenching increases for increasing excitation fluence up to a maximum demagnetization quenching of around 50% at the damage threshold of the sample. This behavior is qualitatively the same for measurements with $\lambda = 400$ nm and $\lambda = 800$ nm, leading to the conclusion that reversal does not occur for TbCo alloy compositions with a quite low Tb concentration.

For $Tb_{26}Co_{74}$ instead, we find that transient reversal of the Co sublattice can occur at high fluence, at least in the measurements with $\lambda = 800$ nm; see Fig. 3(d). However, the demagnetization traces measured at $\lambda = 400$ nm [Fig. 3(c)] show no transient magnetization reversal up to the damage threshold, but complete magnetization quenching occurs. This can be related to the fact that the signal at $\lambda = 400$ nm is a mixture of a contribution coming from the Tb and the Co sublattices, which might cancel each other. Hence, we cannot draw a reliable conclusion concerning the reversal of the Tb sublattice. Here, element-specific measurements using x-ray light sources are needed to disentangle the Tb and Co contributions. Finally, we summarize the results of all fluence-dependent measurements in Fig. 4 more quantitatively. For this purpose we have extracted the quenching of the demagnetization traces and plot it versus the excitation fluence. Note that, strictly speaking, the fluence values for different measurement

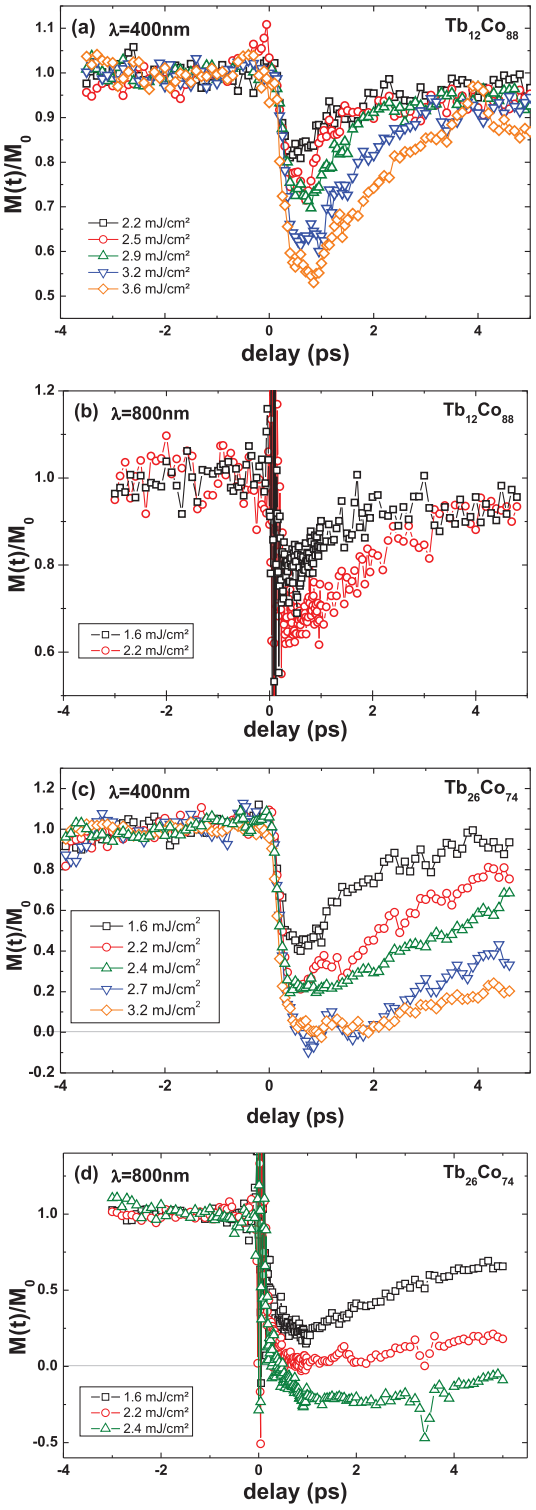

FIG. 3. (Color online) Time dependence of the normalized magnetization, measured with MOKE for different excitation fluences (a) for the $Tb_{12}Co_{88}$ alloy with $\lambda = 400$ nm, (b) for the $Tb_{12}Co_{88}$ alloy with $\lambda = 800$ nm, (c) for the $Tb_{26}Co_{74}$ alloy with $\lambda = 400$ nm, and (d) for the $Tb_{26}Co_{74}$ alloy with $\lambda = 800$ nm. The exciting laser pulses arrive at the sample at the delay of 0 ps. The horizontal gray line marks complete quenching of the magnetization. The spikes around point zero in (b) and (d) are caused by optical artifacts due to the interference of the collinear impinging pump and probe beams having the same wavelength.

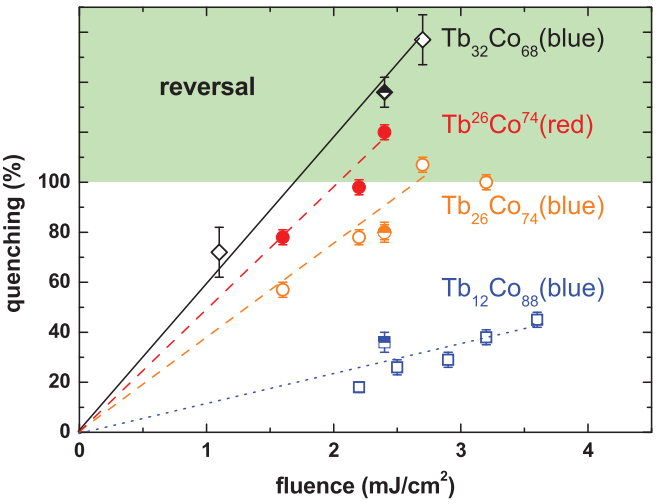

FIG. 4. (Color online) Quenchings extracted from the measurements in Fig. 3 (open symbols for blue probe, closed symbols for red probe). For $Tb_{32}Co_{68}$ we extracted the data points from a measurement for which the demagnetization curves are not explicitly presented in this paper. Additionally the data points for the comparative measurement with the blue probe pulse in Fig. 2(b) are shown (half-filled symbols). Lines are guide to the eye.

series are not comparable. The effective excitation fluence can vary for different measurement series (performed on different days), as the temporal overlap between pump and probe as well as the laser spot profile might slightly change. However, the trends remain valid, as the excitation conditions are constant within a measurement series. Furthermore, the data extracted from the comparative measurements (half-filled data points), where the excitation conditions did not change, show that the deviations are small for the different measurements. Clearly, the increasing quenching with laser fluence becomes visible, as well as the overall higher quenching for increasing Tb concentration. Additionally, one can see that one can drive the magnetization reversal for $Tb_{32}Co_{68}$ just by increasing the excitation fluence.

IV. CONCLUSION

We performed time-resolved MOKE measurements on different TbCo alloys, varying the composition of the alloy and the fluence of the exciting laser pulse. According to Khorsand *et al.* [23], we probed the dynamics with either 400 nm or 800 nm probe pulses to access the Co- and Tb-dominated dynamics. We observed that in constant excitation conditions the magnetization quenching increases if the Tb concentration increases. For $Tb_{32}Co_{68}$ we even observe a subpicosecond transient reversal of the sublattices. We relate the observed increase of the quenching of the Co sublattice with Tb concentration to the enhancement of the spin-orbit coupling and the decrease of the Co-Co exchange coupling with increasing Tb concentration. However, we stress that detailed theoretical investigations on the sublattice magnetization dynamics are needed to really judge the importance of the particular factors. Additionally, successive measurements on different RE-TM alloys, varying the RE and TM material, will help to get deeper insight.

ACKNOWLEDGMENTS

This work was supported by the ANR Project No. ANR-10-BLANC-1005, "Friends," as well as the European Project No. OP2M FP7-IOF-2011-298060 and the Region Lorraine.

[1] H.-P. D. Shieh and M. H. Kryder, Appl. Phys. Lett. **49**, 473 (1986).
[2] M. Aeschlimann, A. Vaterlaus, M. Lutz, M. Stampanoni, and F. Meier, J. Appl. Phys. **67**, 4438 (1990).
[3] M. Aeschlimann, A. Vaterlaus, M. Lutz, M. Stampanoni, F. Meier, H. C. Siegmann, S. Klahn, and P. Hansen, Appl. Phys. Lett. **59**, 2189 (1991).
[4] D. Guarisco, R. Burgermeister, C. Stamm, and F. Meier, Appl. Phys. Lett. **68**, 1729 (1996).
[5] J. Hohlfeld, T. Gerrits, M. Bilderbeek, T. Rasing, H. Awano, and N. Ohta, Phys. Rev. B **65**, 012413 (2001).
[6] C. D. Stanciu, A. Tsukamoto, A. V. Kimel, F. Hansteen, A. Kirilyuk, A. Itoh, and T. Rasing, Phys. Rev. Lett. **99**, 217204 (2007).
[7] T. Ogasawara, N. Iwata, Y. Murakami, H. Okamoto, and Y. Tokura, Appl. Phys. Lett. **94**, 162507 (2009).
[8] C. D. Stanciu, F. Hansteen, A. V. Kimel, A. Kirilyuk, A. Tsukamoto, A. Itoh, and T. Rasing, Phys. Rev. Lett. **99**, 047601 (2007).
[9] K. Vahaplar, A. M. Kalashnikova, A. V. Kimel, D. Hinzke, U. Nowak, R. Chantrell, A. Tsukamoto, A. Itoh, A. Kirilyuk, and T. Rasing, Phys. Rev. Lett. **103**, 117201 (2009).
[10] D. Steil, S. Alebrand, A. Hassdenteufel, M. Cinchetti, and M. Aeschlimann, Phys. Rev. B **84**, 224408 (2011).
[11] S. Alebrand, A. Hassdenteufel, D. Steil, M. Cinchetti, and M. Aeschlimann, Phys. Rev. B **85**, 092401 (2012).
[12] S. Alebrand, M. Gottwald, M. Hehn, D. Steil, M. Cinchetti, D. Lacour, E. E. Fullerton, M. Aeschlimann, and S. Mangin, Appl. Phys. Lett. **101**, 162408 (2012).
[13] K. Vahaplar, A. M. Kalashnikova, A. V. Kimel, S. Gerlach, D. Hinzke, U. Nowak, R. Chantrell, A. Tsukamoto, A. Itoh, A. Kirilyuk, and T. Rasing, Phys. Rev. B **85**, 104402 (2012).
[14] J. M. Li, B. X. Xu, J. Zhang, and K. D. Ye, J. Appl. Phys. **111**, 07D506 (2012).
[15] A. Hassdenteufel, B. Hebler, C. Schubert, A. Liebig, M. Teich, M. Helm, M. Aeschlimann, M. Albrecht, and R. Bratschitsch, Adv. Mater. **25**, 3122 (2013).
[16] S. Mangin, M. Gottwald, C.-H. Lambert, D. Steil, V. Uhlíř, L. Pang, M. Hehn, S. Alebrand, M. Cinchetti, G. Malinowski, Y. Fainman, M. Aeschlimann, and E. E. Fullerton, Nat. Mater. **13**, 286 (2014).
[17] T. Ostler, J. Barker, R. Evans, R. Chantrell, U. Atxitia, O. Chubykalo-Fesenko, S. El Moussaoui, L. Le Guyader, E. Mengotti, L. Heyderman, F. Nolting, A. Tsukamoto, A. Itoh, D. Afanasiev, B. Ivanov, A. Kalashnikova, K. Vahaplar, J. Mentink, A. Kirilyuk, T. Rasing, and A. Kimel, Nat. Commun. **3**, 666 (2012).

[18] I. Radu, K. Vahaplar, C. Stamm, T. Kachel, N. Pontius, H. A. Dürr, T. A. Ostler, J. Barker, R. F. L. Evans, R. W. Chantrell, A. Tsukamoto, A. Itoh, A. Kirilyuk, T. Rasing, and A. V. Kimel, Nature (London) **472**, 205 (2011).

[19] C. La-O-Vorakiat, M. Siemens, M. M. Murnane, H. C. Kapteyn, S. Mathias, M. Aeschlimann, P. Grychtol, R. Adam, C. M. Schneider, J. M. Shaw, H. Nembach, and T. J. Silva, Phys. Rev. Lett. **103**, 257402 (2009).

[20] C. La-O-Vorakiat, E. Turgut, C. A. Teale, H. C. Kapteyn, M. M. Murnane, S. Mathias, M. Aeschlimann, C. M. Schneider, J. M. Shaw, H. T. Nembach, and T. J. Silva, Phys. Rev. X **2**, 011005 (2012).

[21] J. H. Mentink, J. Hellsvik, D. V. Afanasiev, B. A. Ivanov, A. Kirilyuk, A. V. Kimel, O. Eriksson, M. I. Katsnelson, and T. Rasing, Phys. Rev. Lett. **108**, 057202 (2012).

[22] A. J. Schellekens and B. Koopmans, Phys. Rev. B **87**, 020407 (2013).

[23] A. R. Khorsand, M. Savoini, A. Kirilyuk, A. V. Kimel, A. Tsukamoto, A. Itoh, and T. Rasing, Phys. Rev. Lett. **110**, 107205 (2013).

[24] S. Uchiyama, Mater. Chem. Phys. **42**, 38 (1995).

[25] R. Medapalli, I. Razdolski, M. Savoini, A. R. Khorsand, A. Kirilyuk, A. V. Kimel, T. Rasing, A. M. Kalashnikova, A. Tsukamoto, and A. Itoh, Phys. Rev. B **86**, 054442 (2012).

[26] P. Hansen, C. Clausen, G. Much, M. Rosenkranz, and K. Witter, J. Appl. Phys. **66**, 756 (1989).

[27] P. Hansen, S. Klahn, C. Clausen, G. Much, and K. Witter, J. Appl. Phys. **69**, 3194 (1991).

[28] U. Atxitia, J. Barker, R. Chantrell, and O. Chubykalo-Fesenko, arXiv:1308.0993.

[29] V. López-Flores, N. Bergeard, V. Halté, C. Stamm, N. Pontius, M. Hehn, E. Otero, E. Beaurepaire, and C. Boeglin, Phys. Rev. B **87**, 214412 (2013).